

CERN-PPE / 94-155
31 August 1994

Scaling Violation and Fragmentation Functions in $e^+ e^-$ Annihilation

Hermann Fürstenau

*CERN, PPE Division**CH-1211 Geneva 23, Switzerland**invited talk at*

Tennessee International Symposium on

Radiative Corrections: Status and Outlook

June 27- July 1, 1994; Gatlinburg, Tennessee

Abstract

In e^+e^- annihilation, scaling violation has been observed. It is predicted by QCD because the strong coupling α_s is running. A quantitative analysis which uses the precise LEP data has yielded competitive results on α_s . Also, inclusive fragmentation functions have been measured at LEP, and they are compared to heuristic models and recent analytical QCD based calculations. Bottom and charm fragmentation functions are determined at LEP and evidence for scaling violation in the charm fragmentation is observed.

1. Introduction

An e^+e^- collider at $\sqrt{s} = 91\text{GeV}$ is not only an ideal tool to probe the electro-weak standard model, but offers also sensitivity for effects predicted by Quantum Chromodynamic (QCD). Using the precise LEP data, an analysis of scaling violation in e^+e^- yields a quantitative result of the strong coupling α_s , which is competitive with other measurements. QCD also connects the observed hadrons with their quark contents. The quark dynamic can be described by heuristic QCD motivated fragmentation parametrizations. They provide realistic hadron spectra for e^+e^- annihilation which are implemented in Monte Carlo programs. Therefore, a comparison of data and Monte Carlo reflects our understanding of the QCD confinement regime where mesons and baryons are formed. Recent analytical QCD based calculations, in the so-called modified leading logarithm approximation, go beyond a heuristic fragmentation ansatz and provide a more direct comparison of theory with data. The fragmentation properties of hadrons depend on the quark masses which can be studied in the fragmentation of heavy flavours. The heavy flavour

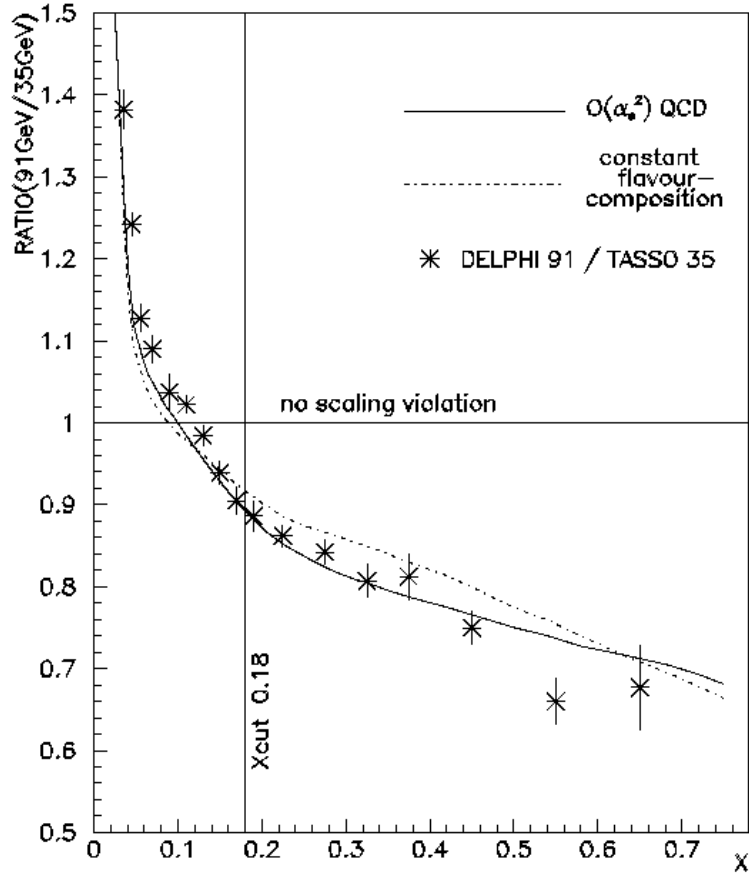


Fig. 1. Ratio of the distributions of the fractional momentum x at $\sqrt{s} = 35 \text{ GeV}$ and at 91 GeV . The dashed-dotted line assumes that the flavour composition at M_Z is the same as at 35 GeV .

fragmentation function for charm and bottom have been measured at LEP and evidence for scaling violation in the charm fragmentation has been observed.

2. Scaling Violation

QCD predicts scaling violation for different processes and was first observed in deep inelastic lepton nucleon scattering. Gluon radiation in the final state is responsible for the deviations from the naive quark-parton model expectations which predicts scaling, i.e. the cross section of the fractional momentum distribution is independent of the energy transfer. In contrast to the space-like regime in lepton nucleon scattering, one also observes in a time-like s-channel process scaling violation i.e. in e^+e^- annihilation. The typical momentum transfer of

$$840 \text{ GeV}^2 \leq Q^2 \leq 8300 \text{ GeV}^2 \quad (1)$$

in e^+e^- is almost one order of magnitude higher than in deep inelastic lepton nucleon scattering when one covers the center of mass energy range from $29 \text{ GeV} \leq \sqrt{s} \leq M_Z$. This high Q^2 range provides an ideal test for QCD where higher twist effects are negligible. Since one is sensitive to gluon radiation, a quantitative determination of the only free parameter in QCD, the strong coupling α_s , can be performed. In order to extract a quantitative value for α_s , one uses

- second order QCD matrix element calculation, and
- fragmentation parametrization.

The second order matrix element Monte Carlo as implemented in JETSET[1] contains a cutoff parameter against infrared and collinear divergences which is carried out by a cutoff, $M_{ij} \geq M_{min}$ where M_{ij} is the invariant mass of two partons i and j^* . Therefore, in order to compare the ‘same’ gluon state at different center of mass energies, M_{min} has to be constant.

The fragmentation parametrization was chosen to be performed by the string fragmentation model[2] which is known to describe even detailed fragmentation properties like the “string effect”[3]. The fragmentation function was chosen[4] to be described by the LUND symmetric fragmentation function[5] for light quarks, and by the Peterson et al. fragmentation function[6] for heavy quarks. As will be shown later, this heavy quark fragmentation function reproduces well the observed inclusive distributions.

Fig. 1 shows the ratio of the distributions of the fractional momentum

$$x = \frac{E_{hadron}}{E_{beam}} \quad (2)$$

at $\sqrt{s} = 35 \text{ GeV}$ [7] and at $\sqrt{s} = M_Z$ [4], where E_{hadron} is the energy of the hadron h in the process $e^+e^- \rightarrow h + X$ and E_{beam} is the beam energy. The full line indicates the QCD prediction in a complete second order calculation. The constant ratio of one shows scaling, the naive expectation in a quark-parton model. Note that the flavour composition and therefore the charm (bottom) fraction changes from 35%(9%) at $\sqrt{s} = 35\text{GeV}$ to 17%(22%) at $\sqrt{s} = 91\text{GeV}$. Fig. 1 shows the influence of a constant flavour composition(dashed-dotted line) compared to the standard model flavour composition(full line). The influence on the scaling violation is small.

To obtain a quantitative value for the strong coupling, one performs a three parameter fit to the data:

- The $\Lambda_{\overline{MS}}$ QCD scale in the \overline{MS} renormalization scheme,

*The actual value is controlled by $y_{min} = M_{min}^2/s$

Uncertainty	$\Delta\Lambda_{\overline{MS}}$
statistical fit uncertainty	$^{+20}_{-11}$ MeV
heavy quark fragmentation	± 10 MeV
independent fragmentation	± 9 MeV
fit range variation	± 10 MeV
$x = 0.08 - 0.18$ to 0.8	
variation of cutoff	± 30 MeV
$M_{ij} = 9 - 18$ GeV	
renormalization scale dependence	± 30 MeV
$\mu^2 = 1 - 0.01 \cdot s$	
	± 60 MeV

Table 1. List of experimental and systematic uncertainties.

- the a parameter of the LUND symmetric fragmentation function with b kept constant, and
- the ϵ_b string fragmentation parameter for b-quarks of the Peterson et al. fragmentation function with $\epsilon_c = 9 \cdot \epsilon_b$.

The uncertainties in this analysis are summarized in Table 1. The final result of this analysis[4] is

$$\alpha_s(M_Z) = 0.118 \pm 0.005 \quad . \quad (3)$$

Recently some next-to-leading order calculations have been performed[8] in order to describe the QCD scaling violation over a wider range of Q^2 . These α_s determinations are still under study (see also the paper of B. Mele in these proceedings).

3. Fragmentation Functions

The scaled momentum spectrum for the process $e^+e^- \rightarrow \text{hadron}^\pm + X$ is shown in Fig. 2 for $\sqrt{s} = M_Z$. The JETSET[1] Monte Carlo is in good agreement with the ALEPH[9] and DELPHI[10] data. The kaon and proton inclusive spectra measured by DELPHI[11] and OPAL[12] are also shown. The kaon spectrum predicted by the JETSET Monte Carlo is slightly softer than the data, however the total production rate agrees well. In case of the protons, the total production rate is overestimated in the Monte Carlo by about 20%. The data appear to have a softer distribution than predicted in the JETSET Monte Carlo. This trend, that meson distributions are better described by Monte Carlo programs than baryons is generally true. The most striking example is the omega production rate which is measured at $\sqrt{s} = M_Z$ to be

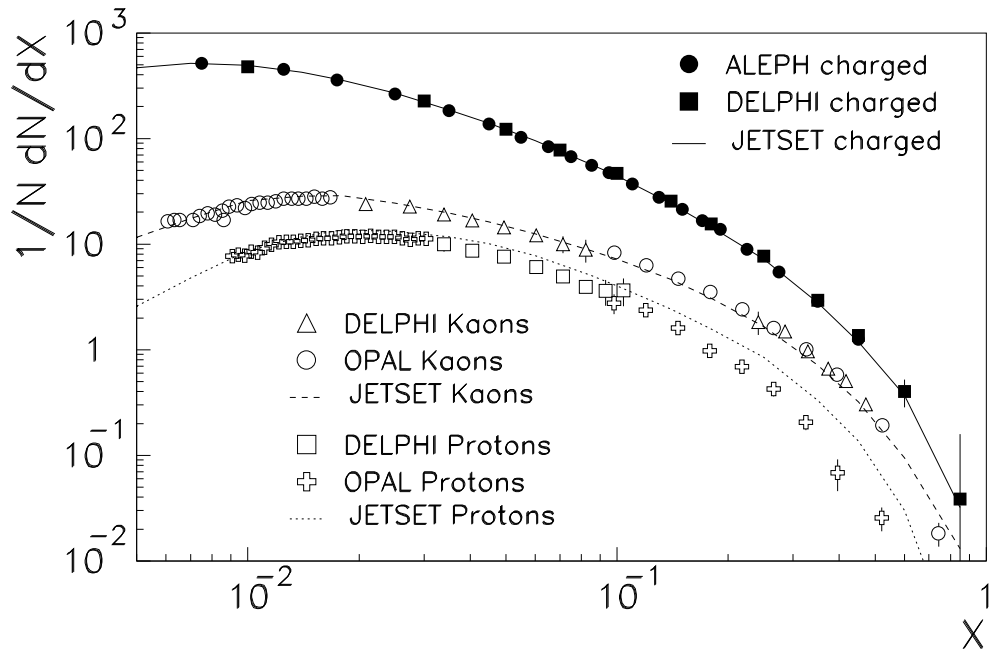


Fig. 2. The total inclusive charged particle spectrum. The pion, kaon and proton spectra are compared with the JETSET Monte Carlo.

0.0050 ± 0.0015 [13]. However, the fragmentation procedure in the JETSET Monte Carlo yields only a rate in the range of $0.00044 - 0.00072$ which is almost one order of magnitude lower. In contrast, the meson production rates are well reproduced[14].

3.1. Analytical Description of Particle Spectra

The Monte Carlo program considered so far uses a heuristic ansatz to describe the fragmentation functions respecting certain physical laws like Lorentz invariance. The number of free parameters in such models is not necessarily small. Another approach tries to explain the particle spectra in the context of the strong force. Of course, pure perturbative QCD cannot be applied for phenomena of the order of the QCD scale Λ . Therefore a Modified Leading Logarithm Approximation (MLLA)[15] was developed to explore this domain. These ‘soft’ QCD calculations make predictions about the inclusive particle spectra. They assume Local Parton Hadron Duality (LPHD) which postulates that locally, parton properties can be observed at hadron level, i.e. after the fragmentation process. The particle spectra are described in terms of the variable

$$\xi = \ln \frac{1}{x} \quad , \quad (4)$$

which transforms the physical x spectrum into a gaussian-like distribu-

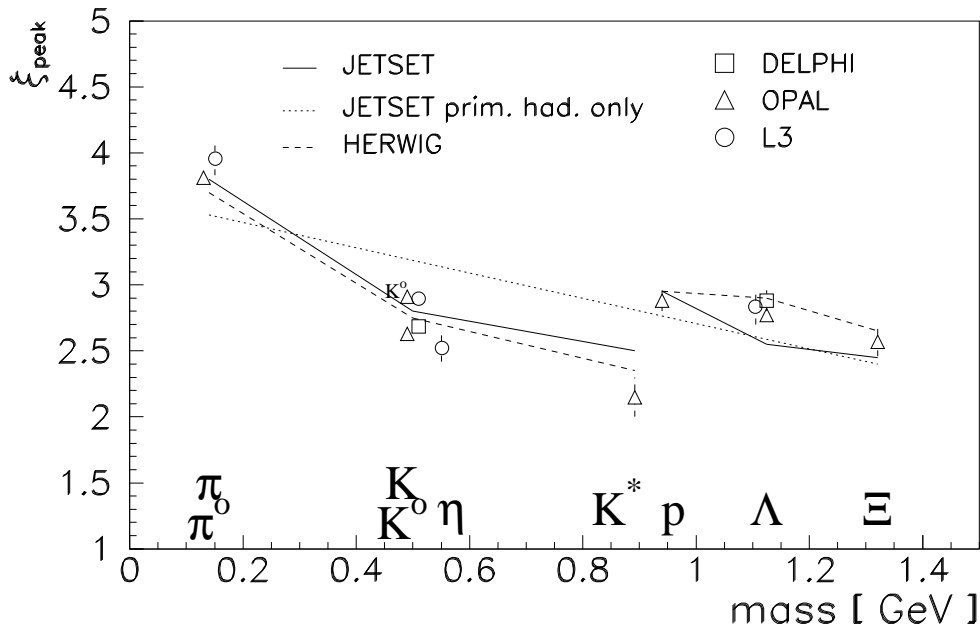


Fig. 3. The ξ_{peak} distribution as a function of the hadron masses measured by DELPHI, L3 and OPAL. The measured points are compared with Monte Carlos.

tion with ξ values typically between 1 and 6. Of particular interest is the absolute maximum of the distribution which defines ξ_{peak} . The MLLA and LPHD make some predictions about ξ_{peak} as a function of \sqrt{s} and the hadron mass:

- ξ_{peak} as a function of the hadron mass for a given center of mass energy is expected to follow approximately a straight line. Fig. 3 shows the ξ_{peak} values measured by DELPHI[11], OPAL[12] and L3[16] as functions of the hadron mass. They are compared with the JETSET[1] and HERWIG[17] Monte Carlo. The measured values cannot be described by a single line. However the individual meson or baryon points could be described by a single line. The ‘gap’ at the $K^*/$ proton threshold is visible. Note that in the LPHD assumption, no particular distinction between meson and baryons is made, which seems to be in disagreement with the data.

The difference between K^0 and K^\pm values of ξ_{peak} is due to decays of heavier particles into K^0 or K^\pm . It should be noted that decay corrections are important for the particle spectra and therefore modify the present picture. For example, if one considers in the JETSET Monte Carlo only hadrons which stem directly from the fragmentation[18], i.e. they are no decay products, than one obtains the dotted line in Fig. 3. This Monte Carlo study shows that the

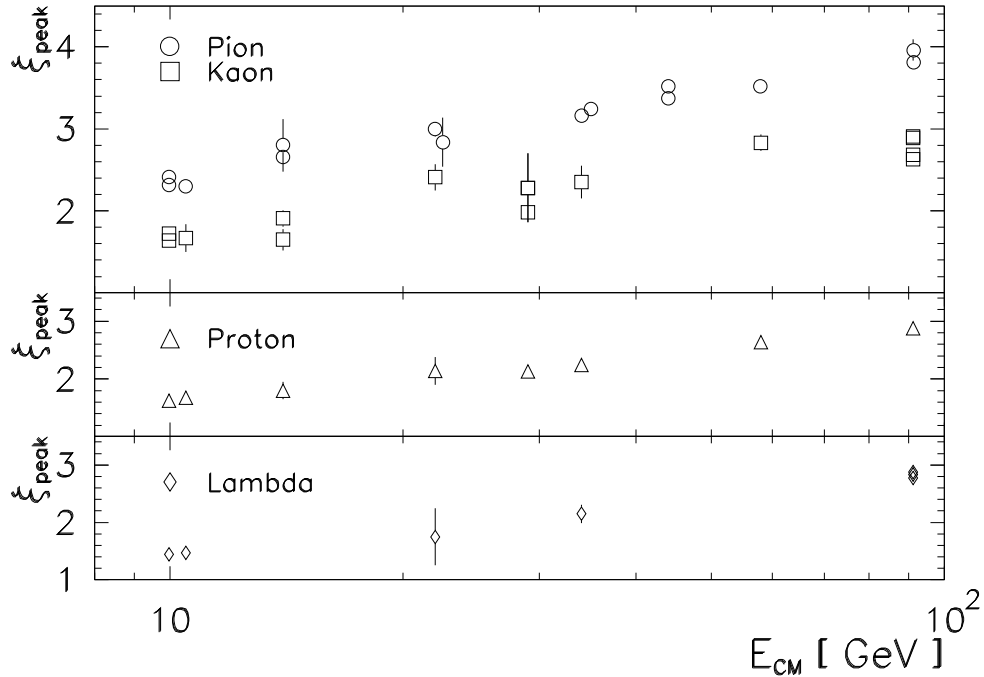


Fig. 4. The ξ_{peak} distribution for different pion, kaon proton and lambdas at different center of mass energies.

‘gap’ between the mesons and baryons disappears and underlines the importance of decays. It is remarkable that the string fragmentation model reproduces the MLLA prediction, since the ansatz is different.

- The calculations predict for a particular hadron, ξ_{peak} as a function of the center of mass energy \sqrt{s} . The prediction is approximately a linear function. Fig. 4 shows the measured distributions for pions, kaons, protons and lambdas as functions of \sqrt{s} . All four measured distributions can be well described by a linear function so that the theoretical prediction is in good agreement with the data. Note that the intercepts and slopes are different for all four distributions so that a general trend cannot be observed.

The MLLA and LPHD make some more precise predictions. A scale of the strong interaction and a normalization factor are free parameters which can be adjusted to the data. In principle this should provide more information. However this qualitative considerations reflects already the main ideas. A more quantitative discussion can be found for example in Ref. [16].

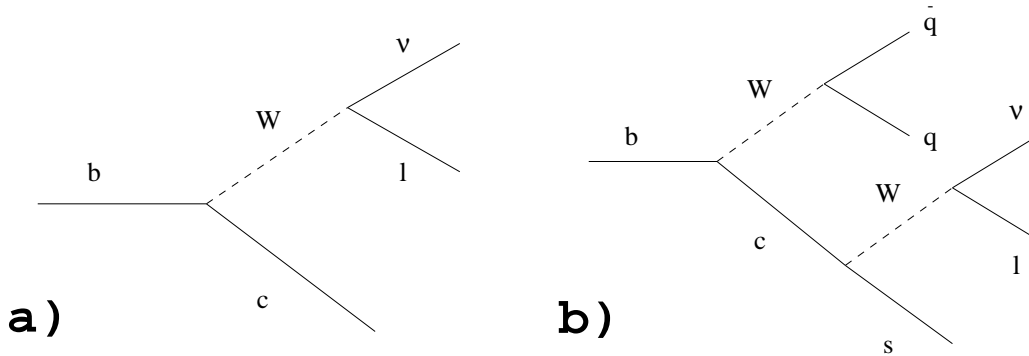


Fig. 5. Feynman diagram of the weak b-quark decays on Born level. Figure a) shows the ‘direct’ lepton production while figure b) shows the cascade lepton production.

4. Bottom Quark Fragmentation Function

Fragmentation functions $f(z)$ are generally expressed in terms of z which is a kind of fractional energy. The exact definition depends on the particular underlying fragmentation model. In the string model one defines:

$$z = \frac{(E + P)_{hadron}}{(E + P)_{parton}}, \quad (5)$$

where the energy E and the momentum P are defined in the quark rest frame. The variable z is unmeasurable! Therefore experimentalists measure the fragmentation function as a function of x which was defined in Eq. 2. In principle this quantity is model independent, however it is defined in the laboratory frame which makes it unattractive from a theoretical point of view.

4.1. Lepton Analysis

The most common method to extract the b quark fragmentation function or the mean x_B for Bottom quarks is the analyses of the semileptonic decay modes of heavy quarks. The Feynman diagrams of these weak decays are shown in Fig. 5. The detected lepton is either an electron or a muon. A two dimensional binned log likelihood fit is performed to the lepton momentum P and the transverse lepton momentum P_t^\ddagger with respect to the jet axis[19]. In the case of events with two leptons, each in a different jet, one can construct a variable $P_c = \sqrt{P_t^2 + P^2}/A$ and

[†]This is an absolute statement. Even a ‘perfect’ detector would not be able to reconstruct unambiguous z .

[‡]The jet direction is determined by excluding the particular lepton from the jet finding algorithm.

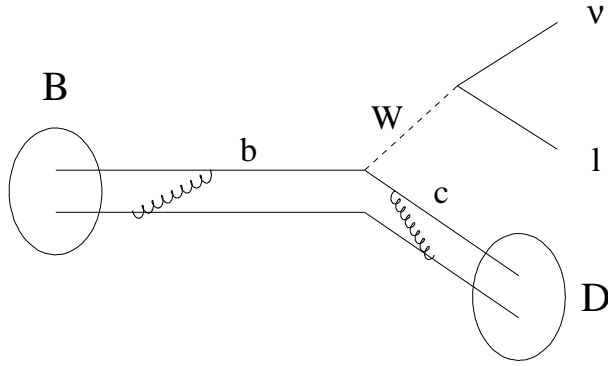


Fig. 6. The schematic semileptonic B-meson decay into a D-meson.

performs the fit to P_c^{min} and P_c^{max} . The best separation is achieved at $A = 1000$.

One usually obtains heavy quark fractions and leptonic branching ratios and the mean $\langle x_B \rangle$ [19, 20, 21, 22] which yields for example [19] $\langle x_B \rangle = 0.702 \pm 0.004 \pm 0.001 \pm 0.009$. The first (second) uncertainty is the statistical (systematic) uncertainty. The last one stems from the semileptonic decay model uncertainty. Two different semileptonic decay models are commonly used:

Altarelli et al. [23] describe the semileptonic decays in a spectator model approach including QCD corrections. The model has two free parameters: the Fermi motion and the quark mass. The values for the parameters were taken for b-decays from CLEO measurements [24] and for c-decays from a fit to DELCO and MARK III [25] data.

Isgur et al. [26] is a form factor model which has in principle no free parameter. However CLEO [24] measured that the relative D^{**} production rate is $\frac{D^{**}}{D+D^*+D^{**}} = 32\%$ which doesn't agree with the 11% obtained from the model. Therefore the rate was adjusted by hand so that the model is now in agreement with the data [25].

From the two decay models one obtains different values for $\langle x_B \rangle$. The spread between the values $\langle x_B \rangle$ in the two models is used to define the decay model dependent uncertainty. This is the largest contribution to the systematic uncertainty while the statistical and experimental uncertainties are much smaller.

4.2. D^* Lepton Analysis

Another method to reconstruct the mean scaled B-meson momentum is to try to reconstruct the individual x_B from its decay products of the reaction:

$$B \rightarrow D + l + \nu \quad , \quad (6)$$

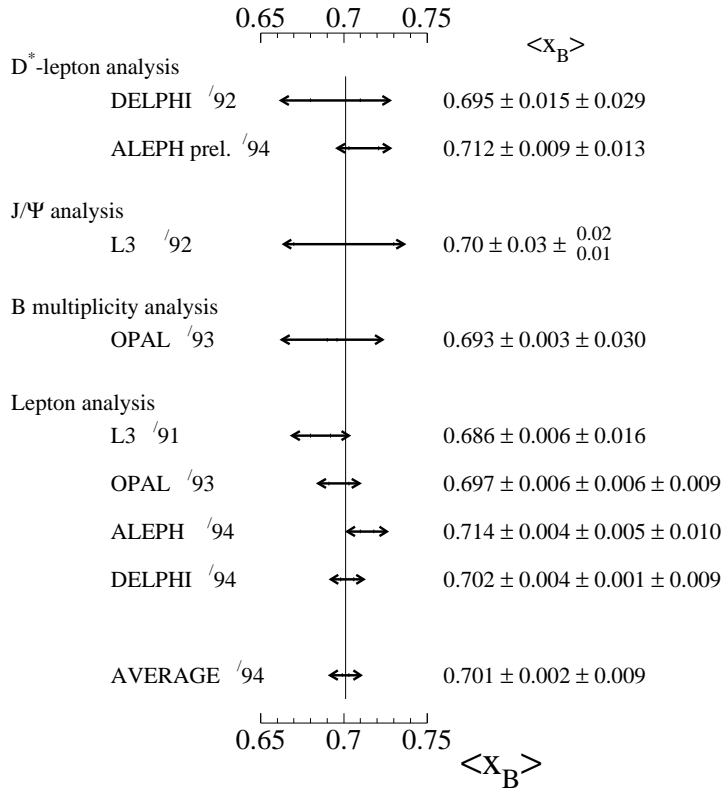


Fig. 7. List of results on $\langle x_B \rangle$ obtained with different methods. The world average value is a weighted average adding experimental, systematic and theoretical uncertainties in quadrature. The total systematic uncertainty is the smallest systematic and theoretical error.

where $B(D)$ is $B(D)$ -meson, l is the lepton and ν is the neutrino (see Fig. 6). The scaled momentum is then defined as:

$$x_B^{reconstruct} = \frac{E_l + E_\nu + E_D}{E_{beam}}, \quad (7)$$

where E_i is the corresponding energy of the particle i /beam. The lepton momentum is determined by the tracking chambers. The neutrino energy is defined as:

$$E_\nu = E_{beam} - E_{vis}^{hemisphere} + \frac{M_{same}^2 - M_{opposite}^2}{4 \cdot E_{beam}}, \quad (8)$$

where $E_{vis}^{hemisphere}$ is the total measured energy in the hemisphere[§]. The invariant mass in the same (opposite) hemisphere as the D , is called M_{same} ($M_{opposite}$). A typical energy resolution[27] is $\Delta E_\nu \approx 1.5 \text{ GeV}$. The

[§]A hemisphere is defined by the Thrust axis

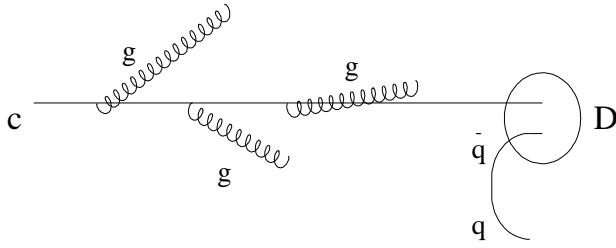


Fig. 8. Schematic view of scaling violation in the D-meson spectrum due to gluon radiation before the meson is formed.

resolution function shows some tails which stem dominantly from neutrons and K_L^0 mesons.

The D-meson is recognized from the decays

- $D^0 \rightarrow K^- \pi^+ (\pi^- \pi^+)$ where the electric charge of the lepton is equal to the charge of the kaon or
- $D^+ \rightarrow K^- \pi^+ \pi^+$.

In case of the production of a $D^{*+} \rightarrow D^0 \pi^+$, E_D is underestimated and E_{vis} is overestimate due to the wrong assignment of the pion energy, when one assumes that the D^0 is the primary meson. This leads to a systematic decrease of x_B . On the other hand, if a pion is not reconstructed due to cracks or other imperfections, the E_{vis} is underestimated which increases x_B . By accident both effects, which are of the order of a couple of percent, almost compensate each other. Nevertheless, a correction for this effect is applied.

In order to obtain an almost Monte Carlo independent result, one applies an iterative procedure for the x_B extraction. The Peterson et al.[6] fragmentation function is assumed in the first step. All Monte Carlo dependent detector corrections are applied and one obtains the measured x_B spectrum. The B-fragmentation function is now reweighted so that it reproduces the measured x_B distribution. After a few cycles the result is stable, and one obtains the preliminary result[27] $\langle x_b \rangle = 0.712 \pm 0.009$.

A summary of different $\langle x_B \rangle$ measurements is shown in Fig. 7. The D^* lepton analysis[27, 28] and the lepton analysis[19, 20, 21, 22] have been discussed above. OPAL[29] and L3[30] also performed two different analysis which lead to larger systematic uncertainties compared to the two methods discussed above. The average value of $\langle x_B \rangle$ over all methods is

$$\langle x_b \rangle = 0.701 \pm 0.002 \pm 0.009 \quad , \quad (9)$$

where the statistical and experimental uncertainty is indicated first and

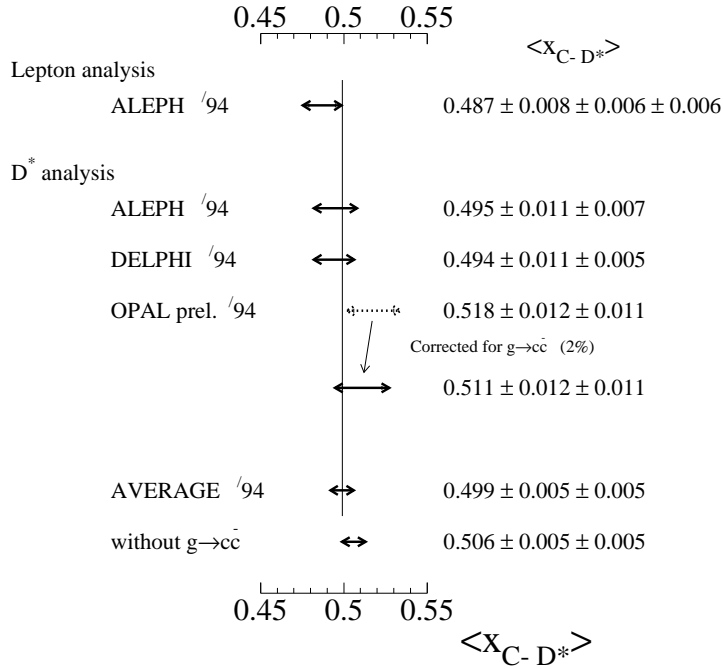


Fig. 9. List of results on $\langle x_C \rangle$ obtained with different method. The average contains the QCD process $g \rightarrow c\bar{c}$. For completeness, the average corrected for this QCD effect is also quoted.

the semileptonic decay model dependence is indicated second.

5. Charm Quark Fragmentation Function

As discussed in the previous section, the D-meson reconstruction provides a sensitive tool for heavy flavour identification. However in case of the charm quark separation, one usually reconstructs the charged D^* from the decay:

$$D^{*+} \rightarrow \begin{matrix} D^0 \pi^+ \\ \hookrightarrow K^- \pi^+ \end{matrix} \quad (10)$$

The ‘direct’ D-meson production from the charm quark is shown in Fig. 8[†]. The $\langle x_{c \rightarrow D} \rangle$ from the ‘direct’ production is harder than from the ‘indirect’ D-meson production of the bottom quark shown in Fig. 6 because a substantial fraction of energy is taken by the W decay into leptons, as shown in the graph, or into quarks. The D^* fraction which stems from the ‘direct’ (‘indirect’) production is called f_c (f_b). The index c (b) indicates the primary flavour. Since $1 = f_c + f_b$, one has to determine for a particular analysis f_b and one obtains therefore $f_c = 1 - f_b$. Four different analysis[31] have been performed in order to extract from Monte

[†]The gluon radiation will be discussed in detail later.

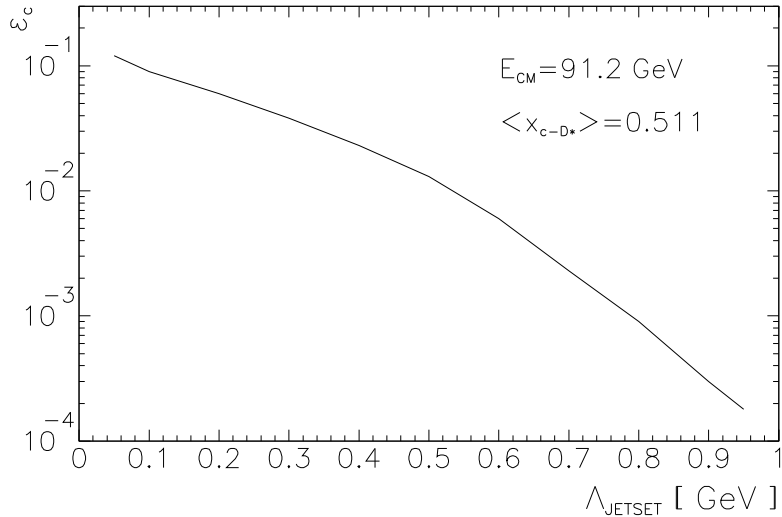


Fig. 10. The Peterson et al. fragmentation parameter as a function of the QCD scale Λ_{JETSET} for constant $\langle x_{c \rightarrow D} \rangle = 0.511$.

Carlo the fractions f_i for a sample of D^* candidates:

- D^* -lepton analysis as discussed above.
- Neural Network analysis which makes use of specific hadronic decay properties.
- Lifetime identification using forward multiplicity of opposite jet as described in Ref. [32].
- D^0 decay length determination with certain flavour dependent characteristics.

All four analysis agree well within the errors and were combined in order to obtain a single f_b fraction. Therefore one determines the measured $x_{c \rightarrow D}$ spectrum with a mean value of

$$\langle x_{c \rightarrow D} \rangle = 0.518 \pm 0.012 \pm 0.011 \quad , \quad (11)$$

where the first uncertainty is a combination of the statistical and experimental uncertainties, while the second one indicates the systematic uncertainty.

An additional contribution of charm quark production comes from gluon splitting $g \rightarrow c\bar{c}$. Therefore the fraction $f_{g \rightarrow c\bar{c}}$ modifies the normalization equation to:

$$1 = f_b + f_c + f_{g \rightarrow c\bar{c}} \quad . \quad (12)$$

The absolute fraction of $f_{g \rightarrow c\bar{c}}$ is not well estimated and depends on the considered Monte Carlo. However for $x_{c \rightarrow D} > 0.2$, the contribution drops

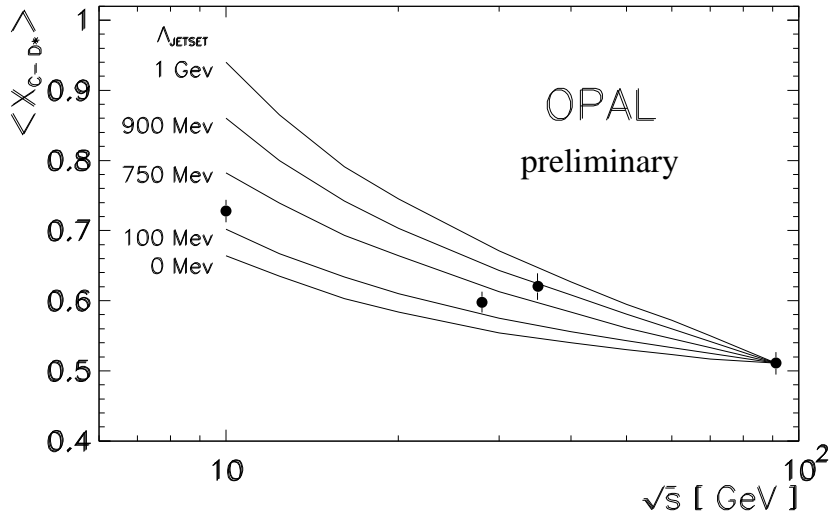


Fig. 11. The $\langle x_{c \rightarrow D} \rangle$ as a function of \sqrt{s} . This shows the first evidence for scaling violation in the charm fragmentation.

from typically 5% to 10% for the total range, to only 1.5%. Since charm quarks from the process $g \rightarrow c\bar{c}$ have a characteristic $1/k$ spectrum, this process influences slightly the $\langle x_{c \rightarrow D} \rangle$ even if the total contribution is small. Most analysis quote a mean value which includes the QCD process. A comparison and averaging of different experiments has to be done consistently. Fig. 9 shows the three D^* results[27, 28, 31] and a lepton analysis. The average $\langle x_{c \rightarrow D} \rangle$ which includes the process of $g \rightarrow c\bar{c}$, is:

$$\langle x_{c \rightarrow D} \rangle = 0.499 \pm 0.005 \pm 0.005 \quad , \quad (13)$$

where the first uncertainty is a combination of the statistical and experimental uncertainties, while the second one indicates the systematic uncertainty. Note that the systematic error is almost half of the total systematic uncertainty of the $\langle x_b \rangle$ measurement. This is due to the fact that the semileptonic decay model uncertainty is absent in the charm quark analysis.

5.1. Scaling Violation of Charm

For practical purposes, it is useful to know the particular fragmentation parameter ϵ_c of the Peterson et al. fragmentation[6]. However if one tries to determine its value, one notices a significant dependence on the choice of the QCD scale Λ . For $\langle x_{c \rightarrow D} \rangle = 0.511$, Fig. 10 shows ϵ_C as a function of Λ_{JETSET} , the leading order QCD scale used in the JETSET Monte Carlo[1]. This means, every point on the curve $(\Lambda_{JETSET}, \epsilon_c)$ reproduces the same $\langle x_{c \rightarrow D} \rangle$. This can be explained by the sensitivity

of $\langle x_{c \rightarrow D} \rangle$ to gluon radiation before the charmed meson is formed (see Fig. 8). Therefore, if one wants to characterize the fragmentation properties of charm, one should quote $\langle x_{c \rightarrow D} \rangle$ rather than ϵ_c or Λ_{JETSET} ! This statement is also valid for bottom fragmentation.

If one considers the $\langle x_{c \rightarrow D} \rangle$ as a function of \sqrt{s} (see Fig. 11) [31, 33, 34, 35, 36, 37] one observes that $\langle x_{c \rightarrow D} \rangle$ is not constant. This can be interpreted as scaling violation. The lines in Fig. 11 show the Monte Carlo behaviour for different leading order QCD scales Λ_{JETSET} . The Monte Carlo curve with $\Lambda_{JETSET} = 0$ MeV shows simply the phase space effects. This is the first evidence for scaling violation in the charm fragmentation.

6. Summary

Scaling violation in e^+e^- has been observed and quantitative results can be obtained for the strong coupling $\alpha_s(M_Z) = 0.118 \pm 0.005$. The measured fragmentation functions of mesons in e^+e^- are well reproduced by Monte Carlo programs using heuristic models. However some significant deviations have been found for the baryon spectra. An analytical ansatz in the framework of MLLA and LPHD to describe fragmentation functions as a function of \sqrt{s} is in agreement with the data. A coherent picture of mesons and baryons can be achieved by taking hadron decays into account. The heavy flavour bottom (charm) fragmentation function has been measured at $\sqrt{s} = 91.2 \text{ GeV}$ with $\langle x_b \rangle = 0.701 \pm 0.002 \pm 0.009$ ($\langle x_{c \rightarrow D} \rangle = 0.499 \pm 0.005 \pm 0.005$). Evidence for scaling violation of $\langle x_{c \rightarrow D} \rangle$, i.e. in the charm fragmentation, as a function of the center of mass energy is observed.

7. Acknowledgements

I would like to thank Siggie Bethke, Otmar Biebel, Wim de Boer, Ian Brock, Bob Clare, Paul Colas, Alessandro De Angelis, Alex Firestone, Giorgio Gratta, Michael Hauschild, Klaus Mönig, Jean Pierre Lees, Peter Maettig, Torbjorn Sjostrand and Wilbur Venus.

1. T. Sjöstrand, *Comp. Phys. Comm.* **27** (1982) 243, *ibid.* **28** (1983) 229; T. Sjöstrand and M. Bengtsson, *Comp. Phys. Commun.* **43**(1987)367.
2. X. Artru, G. Mennessier, *Nucl. Phys.* **B70** (1974) 93; B. Anderson, G. Gustafson, G. Ingelman, T. Sjöstrand, *Phys. Rep.* **97** (1983) 31.
3. JADE Collab., W. Bartel et al., *Phys. Lett.* **B101** (1981) 129.

^{||}In principle, ϵ_c and Λ_{JETSET} determine also the fragmentation properties. However this seems inconvenient.

4. DELPHI Collab., P. Abreu et al., *Phys. Lett.* **B311** (1993) 408.
5. M.G. Bowler, *Z. Phys.* **C11** (1981) 169; B. Andersen, G. Gustafson, B. Söderberg, *Z. Phys.* **C20** (1983) 317; D.A. Morris, *Nucl. Phys.* **B313** (1989) 634.
6. C. Peterson, D. Schlatter, I. Schmitt, P.M. Zerwas, *Phys. Rev.* **D27** (1983) 105.
7. TASSO Collab., W. Braunschweig et al., *Z. Phys.* **C47** (1990) 187.
8. P. Nason, B.R. Webber, CERN preprint *CERN-TH 7018/93* (1993).
9. ALEPH collaboration, D. Decamp et al., *Phys. Lett.* **273B** (1992) 253.
10. DELPHI collaboration, P. Aarnio et al., *Phys. Lett.* **240B** (1990) 271.
11. DELPHI collaboration, internal note, *DELPHI/94-49 Phys 371*, March 1994, submitted to Glasgow HEP conference, **gls-0182**.
12. OPAL collaboration, R. Akers et al., *CERN-PPE/94-017*, submitted to *Zeit. Phys.*.
13. OPAL Collab., P.D. Acton et al., *Phys. Lett.* **B291** (1992) 503.
14. A. De Angelis, *J. Phys.* **4** (1993) 1233.
15. Y.L. Dokshitzer, V.S. Fadin, V.A. Khoze, *Phys. Lett.* **115B** (1982) 242, Y.L. Dokshitzer, V.S. Fadin, V.A. Khoze, *Zeit. Phys.* **C15** (1982) 325, Y.I. Azimov, Y.L. Dokshitzer, V.A. Khoze, S.I. Troyan, *Zeit. Phys.* **C27** (1985) 65, Y.L. Dokshitzer, V.A. Khoze, C.P. Fong, B.R. Webber, *Phys. Lett.* **273B** (1991) 319. Y.L. Dokshitzer, V.A. Khoze, A.H. Mueller, S.I. Troyan, 'Basic of Perturbative QCD', editions Frontiers, Gif-sur-Yvette, France, (1991) Y.L. Dokshitzer, V.A. Khoze, S.I. Troyan, *Journ. Mod. Phys.* **A7** (1992) 1875, Y.L. Dokshitzer, V.A. Khoze, S.I. Troyan, *Zeit. Phys.* **C55** (1992) 107.
16. L3 collaboration, A. Adam et al., *CERN-PPE/94-053*, submitted to *Phys. Lett.*.
17. G. Marchesini, B.R. Webber, *Nucl. Phys.* **B238** (1984) 1; G. Marchesini, B.R. Webber, *Nucl. Phys.* **B310** (1988) 461; G. Marchesini, B.R. Webber, *Nucl. Phys.* **B330** (1990) 261; G. Marchesini, B.R. Webber, *Nucl. Phys.* **B349** (1991) 635.
18. OPAL collaboration, R.J Hemingway, internal note, June 1994, submitted to Glasgow HEP conference, **gls-0483**.
19. DELPHI collaboration, internal note, *DELPHI/94-62 Phys 383*, June 1994, submitted to Glasgow HEP conference, **gls-0178**.
20. L3 collaboration, O. Adeva et al., *Phys. Lett.* **B261** (1991) 177.
21. OPAL collaboration, R. Akers et al., *Zeit. Phys.* **C60** (1993) 199.
22. ALEPH collaboration, D. Buskulic et al., *CERN-PPE/94-017*, submitted to *Zeit. Phys.*.
23. G. Altarelli et al., *Nucl. Phys.* **B208** (1982) 365.

24. CLEO collaboration, S. Henderson et al. *Phys. Rev.* **D45** (1992) 2212.
25. The LEP Electroweak Working Group, *DELPHI/94-23 Phys* **357**, March 1994.
26. N. Isgur et al., *Phys. Rev.* **D39** (1989) 799.
27. ALEPH collaboration, I. Debonis, J.P. Lees, preliminary internal ALEPH note, submitted to Glasgow HEP conference, **gls-0581**.
28. DELPHI collaboration, P. Abreu et al., *Zeit. Phys.* **C57** (1993) 181.
29. OPAL collaboration, R. Akers et al., *Zeit. Phys.* **C61** (1993) 209.
30. L3 collaboration, O. Adriani et al., *Phys. Lett. B288* (1992) 412.
31. OPAL collaboration, preliminary Physics Note *PN 131*, March 25, 1994. submitted to Glasgow HEP conference, **gls-0513**.
32. OPAL collaboration, R. Akers et al., *Zeit. Phys.* **C61** (1994) 357.
33. ARGUS collaboration, H. Albrecht et al., *Z. Phys.* *C52* (1991) 35.
34. HRS collaboration, P. Baringer et al., *Phys. Lett. B 206* (1988) 551.
35. DELCO collaboration, H. Yamamoto et al., *Phys. Rev. Lett.* *54* (1985) 522; TPC/Two-Gamma collaboration, H. Aihara et al., *Phys. Rev. D 34* (1986) 1945.
36. TASSO collaboration, W. Braunschweig et al., *Z. Phys.* *C44* (1989) 367.
37. JADE collaboration, W. Bartel et al., *Phys. Lett. B 146* (1984) 121.